Original research article

EJO European Journal of Ophthalmology

European Journal of Ophthalmology
2023, Vol. 33(3) 1434–1442

DOI: 10.1177/11206721221144477
journals.sagepub.com/home/ejo
SAGE

Ageing changes in retinal outer nuclear layer thickness and cone photoreceptor density using adaptive optics-free imaging

Juliane Matlach[1,2,3], Padraig Mulholland[1,4,5], Marketa Cilkova[1], Reena Chopra[1], Nilpa Shah[1], Tony Redmond[5], Steven C Dakin[1,6], David F Garway-Heath[1] and Roger S Anderson[1,4]

Abstract

Purpose: To investigate age-related changes of the outer nuclear layer (ONL) thickness and cone density, and their associations in healthy participants using a modified, narrow scan-angle Heidelberg Retina Angiograph (HRA2).

Methods: Retinal cones were imaged outside the fovea at 8.8° eccentricity and cone density was compared to ONL thickness measurements obtained by Spectral-Domain Optical Coherence Tomography (SD-OCT) at the same locations. Fifty-six eyes of 56 healthy participants with a median age (interquartile range, IQR) of 37 years (29–55) were included.

Results: Median (IQR) cone count was 7,472 (7,188, 7,746) cones/mm^2 and median (IQR) ONL thickness was 56 (52, 60) µm for healthy participants. Both cone density and ONL thickness were negatively associated with age: cone density, $R^2 = 0.16$ ($F(1,54) = 10.41$, $P = 0.002$); ONL thickness, $R^2 = 0.12$ ($F(1,54) = 7.41$, $P = 0.009$). No significant association was seen between cone density and ONL thickness ($R^2 = 0.03$; $F(1,54) = 1.66$, $P = 0.20$).

Conclusion: Cone density was lower, and ONL thinner, in older compared to younger participants, therefore, image-based structural measures should be compared to age-related data. However, cone density and ONL thickness were not strongly associated, indicating that determinants of ONL thickness measurements other than cone density measurements, and including measurement error, have a major influence.

Keywords

Cone imaging, outer nuclear layer, OCT, imaging

Date received: 3 May 2022; accepted: 21 November 2022

Introduction

With the advancement of technology for imaging the eye, not only has it become commonplace to resolve and measure retinal layers *in vivo*, but, increasingly, resolution is reaching single cell level.[1] High-resolution adaptive optics (AO) devices allow for imaging of retinal cells, e.g., a detailed view of the cone photoreceptor mosaic.[2–6] With suitable modifications, the Heidelberg Retina Angiograph (HRA; Heidelberg Engineering GmbH, Heidelberg, Germany), a confocal laser ophthalmoscope, also allows *in vivo* imaging of the cone photoreceptor mosaic in the clinic.[7] Specifically when the scan angle of

[1]NIHR Biomedical Research Centre, Moorfields Eye Hospital & UCL Institute of Ophthalmology, London, UK
[2]Department of Ophthalmology, University Medical Center, Johannes Gutenberg University Mainz, Mainz, Germany
[3]Department of Ophthalmology, University of Leipzig, Leipzig, Germany
[4]Vision Science Research Group, Ulster University, Coleraine, UK
[5]School of Optometry and Vision Sciences, Cardiff University, Cardiff, UK
[6]School of Optometry & Vision Science, The University of Auckland, Auckland, New Zealand

Corresponding author:
Juliane Matlach, Department of Ophthalmology, University of Leipzig, Leipzig, Germany.
Email: juliane.matlach@medizin.uni-leipzig.de

the instrument is reduced well below that of its commercial specification, a fast and non-invasive method of high-resolution imaging is achievable, with minimal discomfort to patients, enabling *in vivo* images of the cone photoreceptor mosaic and the possibility of identifying and quantifying pathological cone loss. However, in order to disentangle the contributions of pathology and normal ageing to any identified cone loss, with this instrument, it is necessary to firstly quantify the association between cone density measurements and age in healthy individuals.[8–10]

In studies of photoreceptor degeneration in retinal disease, the outer nuclear layer (ONL), automatically segmented by Spectral-Domain optical coherence tomography (SD-OCT), has been proposed as a surrogate for photoreceptor loss.[11,12] ONL thinning has been observed in eyes with retinitis pigmentosa[11] and Stargardt disease.[12] This disruption of the ONL and deeper layers has been observed in areas with low cone count as determined with AO technology.[12] However, this was not confirmed by other studies reporting normal or thicker ONL in retinitis pigmentosa and geographic atrophy due to cell swelling.[13,14] Also, in eyes without retinal degeneration, when OCT data were compared to histological sections, the ONL near the fovea was found to be thicker, rather than thinner as might be expected with age-related photoreceptor loss.[15] The ONL may actually be thicker in elderly participants due to structural changes within the retina, such as Müller cell hypertrophy, a result of photoreceptor loss with age, observable with OCT and confirmed in histological retinal sections of human donor eyes.[15] Another AO study of healthy participants found that the ONL (measured with OCT) became thicker with age, but that cone packing density, measured with AO, was lower. In addition to Müller cell hypertrophy, a thicker ONL with age may also be a result of retinal remodeling.[16,17] With the ability to more directly measure photoreceptor density in a clinical situation, a surrogate measure such as the thickness of a retinal layer, may no longer be required or indeed useful.

The aim of this study is to investigate a) the association between cone density, as measured with a modified small-angle adaptive optics-free HRA2, and age, b) the association between ONL thickness, measured and automatically segmented with a SD-OCT, and age, as well as c) the association between cone density and ONL thickness in healthy participants.

Methods

The study protocol was approved by the National Health Service (NHS) National Institute for Health Research Ethics Committee Clinical Research Network North Thames, London, UK and the University College London (UCL) Research Ethics Committee, London, UK (IRAS reference: 116000, Study ID: 15890). The research followed the tenets of the Declaration of Helsinki. Written informed consent was obtained from all participants prior to inclusion.

Participants

Fifty-six eyes of 56 healthy participants with a median [interquartile range, IQR] age of 37 [29, 55] years were examined. Median [IQR] sphere was −0.50 [−1.50, +0.50] D with a range from −6.50 to +2.25 D, and median [IQR] astigmatism was −0.25 [−0.50, 0.00] D with a range from −4.00 to 0.00 D. All participants had an optic nerve rim area within normal limits according to the Moorfields Regression Analysis on the Heidelberg Retina Tomograph (HRTII; Heidelberg Engineering GmbH, Heidelberg, Germany) and/or overall normal peripapillary retinal nerve fiber layer (RNFL) on SD-OCT (Spectralis OCT, Heidelberg Engineering GmbH, Heidelberg, Germany), as well as a full visual field, determined by Standard Automated Perimetry (SAP; Humphrey Field Analyzer, HFAII; Carl Zeiss Meditec, Dublin, CA, Swedish Interactive Threshold Algorithm 24–2 strategy). All participants had reliable visual field results with fewer than 30% fixation losses and a false-positive rate less than 15%, stable intraocular pressure less than 21 mmHg, and visual acuity equal to, or better than, 20/30 (6/9) in the test eye. Exclusion criteria were evidence of any ocular or systemic disease, eye surgery, or laser treatment that could affect otherwise normal retinal architecture. The right eye was chosen if both eyes were suitable for inclusion. Fifty-one right eyes and 5 left eyes were included.

Cone imaging with a modified small-angle HRA2 and image analysis

All participants underwent *in vivo* cone imaging with a modified small-angle HRA2 and a standard SD-OCT. Imaging was performed by an experienced operator (JM). As in a previous study by our group,[7] the scan angle of a standard HRA2 (Heidelberg Engineering GmbH, Heidelberg, Germany) was reduced to 3° and the fixation control array modified in order to image cones *in vivo* without the use of AO technology. Cones were imaged in each of the supero- and infero-nasal, and supero- and infero-temporal quadrants at 8.8° retinal eccentricity (Figure 1). The scan field was $3° \times 3°$ which is equivalent to 0.825×0.825 mm on the retina at that location, based on the conversion method of Drasdo and Fowler.[18]

Image analysis

An in-depth description of the modified HRA2, acquisition of images, and cone counts can be found in our previously

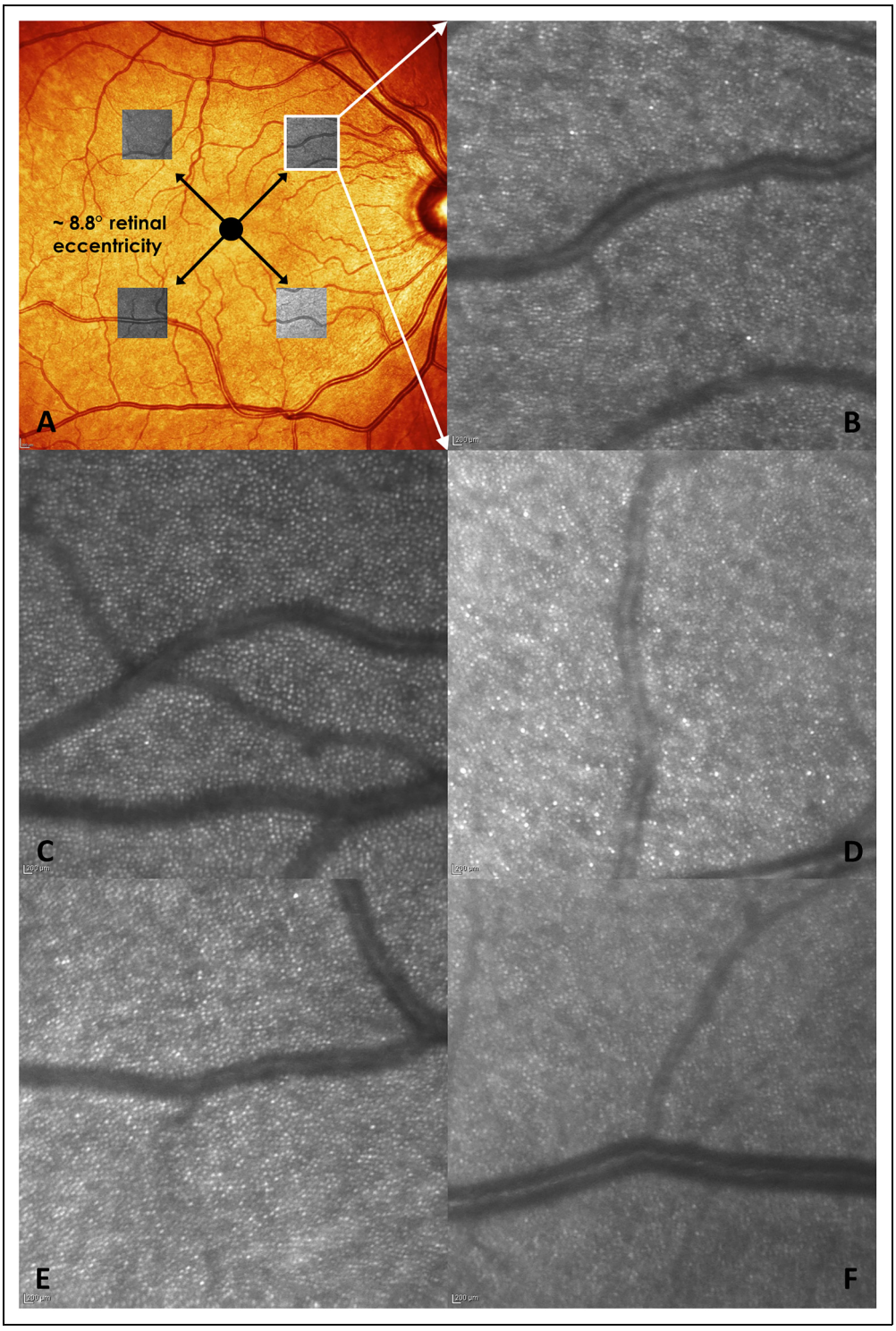

Figure 1. *In vivo* cone imaging with an adaptive optics-free small-angle Heidelberg retina angiograph 2.
Fundus image of a 58-year old healthy participant with superimposed cone scans performed at 4 retinal locations at approximately 8.8° foveal eccentricity (a) and cone image (b). Examples of cone imaging of a 21-yearold (c), 37-year old (d), 42-year old (e), and a 65 year-old healthy participant (f).

published study.[7] In short, cones were identified by the method of Li & Roorda[19] in MATLAB (R2014b) with the image processing toolbox (IPT). The first analysis applies a low-pass filter in the frequency domain to remove high-frequency noise from the image. The image is then converted back to the spatial domain and the local

luminance maxima are detected using the IPT function *imregionalmax*. These identified regions were assumed to be cone centers and were plotted as single white pixels on a black background. Binary blobs were dilated using a white disk of diameter appropriate to ensure the identified cones were not closer than physiologically possible. Following this, each remaining spatially independent blob was counted as a cone. This value was then converted to cone density as cones/mm^2. Although this method has been shown to provide cone density estimates that are very similar to those determined through manual counts, with the spatial localization of identified cones also being accurate for images acquired with AO technology, some cones may be missed even in high quality scans.[19–21]

A total of 203 scans of 224 locations were included for the final calculation of cone density. This represented more than 90% of scans. Poor quality scans (where no cones could be resolved within the scan window, owing to excessive movement, lens opacity, or poor participant cooperation) were excluded from analysis. These 21 excluded scans were not all from older participants.

ONL thickness

ONL thickness was measured and automatically segmented with SD-OCT posterior pole grids (Spectralis OCT, acquisition software version 5.7.4.0). The grids on the posterior pole scans were rotated and translated to align with individual cone images, and then moved to match the position of the cone images by using specific landmarks, for example blood vessels (Figure 2). Single posterior pole grids of ONL thickness had the same scan width of 3° × 3° as the cone scans.

Statistical analysis

Statistical analyses were performed with SPSS 23 (IBM Corporation, Armonk, NY, USA). Median [IQR] values and percentage splits were calculated for demographic data (age, gender, eye, refraction), cone density, and ONL thickness, as appropriate. Ordinary least squares linear regression was used to test the association between structural measurements and age, as well as the association between individual structural measurements. A P-value of <0.05 was considered statistically significant.

Results

Table 1 shows the demographics for all healthy participants.

Cone density as a function of age

Figure 1 shows examples of cone scans in healthy female participants aged 58 (A, B) and 21 (C, D) years. Median [IQR] cone density across all participants was 7,472 [7,188, 7,746] cones/mm^2 (Table 2). There was a statistically significant association between cone density and age ($F(1,54) = 10.41$, $P = 0.002$), with modest strength ($R^2 = 0.16$). Cone density was negatively associated with age with a slope of −11.54 cones/mm^2 per year (Figure 3(a) and (b)).

ONL thickness as a function of age

Median [IQR] ONL thickness for the entire cohort was 56 [52, 60] μm (Table 2). There was a statistically significant association between ONL thickness and age ($F(1,54) = 7.41$, $P = 0.009$), however the strength of the association was modest ($R^2 = 0.12$). ONL thickness was negatively correlated with age, with a slope of 0.14 μm per year (Figure 3(c) and (d)).

Association between cone density and ONL thickness

There was no statistically significant association between cone density and ONL thickness ($F(1,54) = 1.66$, $P = 0.20$, $R^2 = 0.03$, slope = 0.002, Figure 4).

Discussion

In this study, we report the association between age and structural measures of the outer retina (cone density and ONL thickness), as measured with a modified scanning laser ophthalmoscope and SD-OCT, centered at 8.8° retinal eccentricity. We also investigated the relationship between cone density and ONL thickness. We used a modified small-angle HRA2, without AO technology, to capture high-resolution images of the cone photoreceptor mosaic. This novel technique allows fast and non-invasive scans of retinal cones.

In the current study, we found a statistically significant negative correlation between cone density and age. This finding is in contrast to that reported in an AO study by Song *et al*[10] where, although cone packing was negatively associated with age within 0.5 mm of the fovea, beyond that eccentricity, cone density was independent of age. Song *et al* found a cone density of approximately 8,600 cones/mm^2 at 2.6 mm eccentricity in two separate age groups (22–35 years and 50–65 years).[10] Muthiah et al imaged out to 7° retinal eccentricity, finding 13,000 cells/mm^2 at 7° and concluded that their results agree with those of other studies.[22] Histological data by Curcio et al reported cone counts of approximately 9,700 cones/mm^2 at 2.5 mm retinal eccentricity in younger donors.[23] Accounting for small differences in eccentricity between studies, our mean cone counts are slightly smaller than those reported in AO and histological studies of cone number and density. However, given the between-study variability in cone counts, this difference would not be

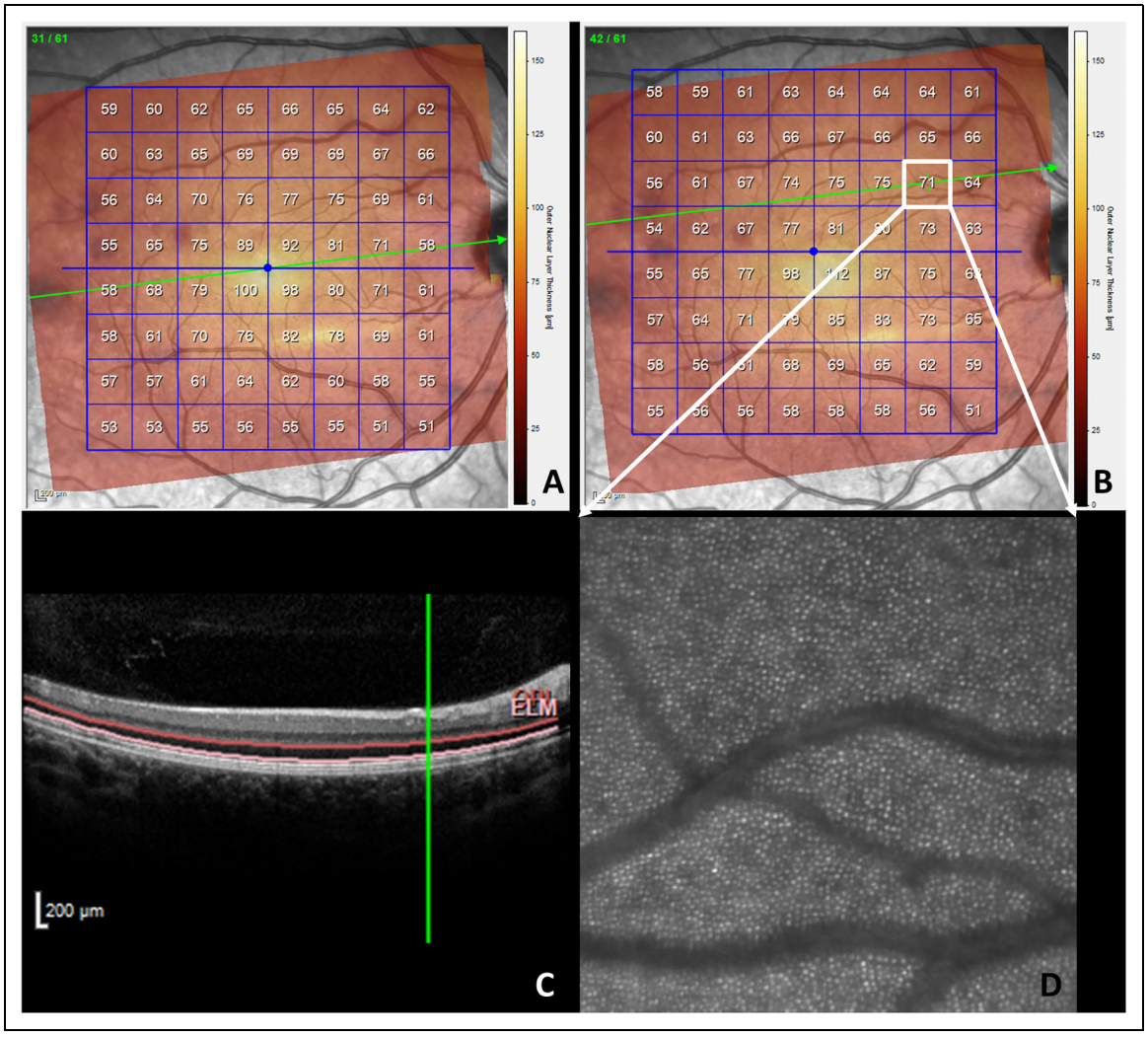

Figure 2. Adjustment of outer nuclear layer (ONL) thickness measurement.
False-colour thickness map of the automated ONL measurement (posterior pole grid) was rotated to a straight square on the fundus image (a). The posterior pole grid was subsequently moved to match the position of the cone images by using specific landmarks, for example blood vessels (b). The numbers at the center of each box display the average ONL thickness in that box which changed after moving when different areas are covered. Horizontal SD-OCT scan and automated segmentation of the ONL at the location of the cone scan (c) which is displayed in (d). Note: Segmentation errors were manually corrected.

Table 1. Characteristics of healthy participants.

n of eyes/ participants	56
Age, years	37 [29, 55] min-max 21–68
Sex, male/female	18/38 (32/68)
Eye, right/left	51/5 (91/9)
Spherical error, DS	−0.50 [−1.50, +0.50] range −6.50 to +2.25
Cylindrical error, DC	−0.25 [−0.50, 0.00] range −4.00 to 0.00

Data are absolute vales (%) and medians [IQR] as appropriate.
DC, diopter cylinder; DS diopter sphere; IQR interquartile range; n number of eyes/participants.

considered unreasonable. The algorithm used for automated cone counting in our study was based on previous work for cone images captured with AO devices which also found good agreement between manual and automated cone counting.[19,22] In our previous study, we discussed why our cone count appears to be lower than reported in other studies.[7] Refractive error, age, variability of eccentricity, and retinal magnification may be possible factors for differences in cone density between our study and those of others. Our method has, however, been previously shown to be robust to simulated lens opacity.[24] We have also compared cone counts generated by the automated algorithm (used in this study) with a manual analysis technique, and found no meaningful difference.[20]

In addition to the negative correlation between cone count and age, we also found a negative correlation between ONL thickness and age. This is somewhat at odds with previously published reports of a positive association between ONL thickness and age.[15,16] It has been argued that a thicker ONL can be attributed to remodeling of the retina in the elderly, and in degenerative diseases. Gliosis of retinal cells within the boundaries used for ONL measurements with OCT, in addition to neurite sprouting of bipolar and horizontal cells and Müller cell hypertrophy, or a misleading signal from Henle fibers in the foveal region, may be possible changes occurring in the degenerating retina.[17,25] The ONL may be helpful as a biomarker for photoreceptor loss when studying photoreceptor degeneration in retinal diseases like retinitis pigmentosa, Stargardt's disease or other macular degeneration.[11,12] However, evidence from the literature is still inconclusive, following reports of a 'normal' or even thicker ONL in degenerative diseases.[13,14] Chui et al reported that older participants had a lower cone count but a thicker ONL around the fovea, compared to younger controls.[16] However, ONL thickness, as well as cone density, decreases with retinal eccentricity, becoming

Table 2. Cone density and ONL thickness for each retinal location.

Cone density in cones/mm^2	
Superior nasal	7639 [7205, 8075]
Inferior nasal	7460 [6864, 7811]
Superior temporal	7614 [7092, 7895]
Inferior temporal	7329 [6971, 7631]
Overall	7472 [7188, 7746]
ONL thickness in µm	
Superior nasal	60 [56, 65]
Inferior nasal	53 [50, 59]
Superior temporal	59 [55, 61]
Inferior temporal	54 [49, 59]
Overall	56 [52, 60]

Data are medians [IQR].
IQR interquartile range; ONL outer nuclear layer.

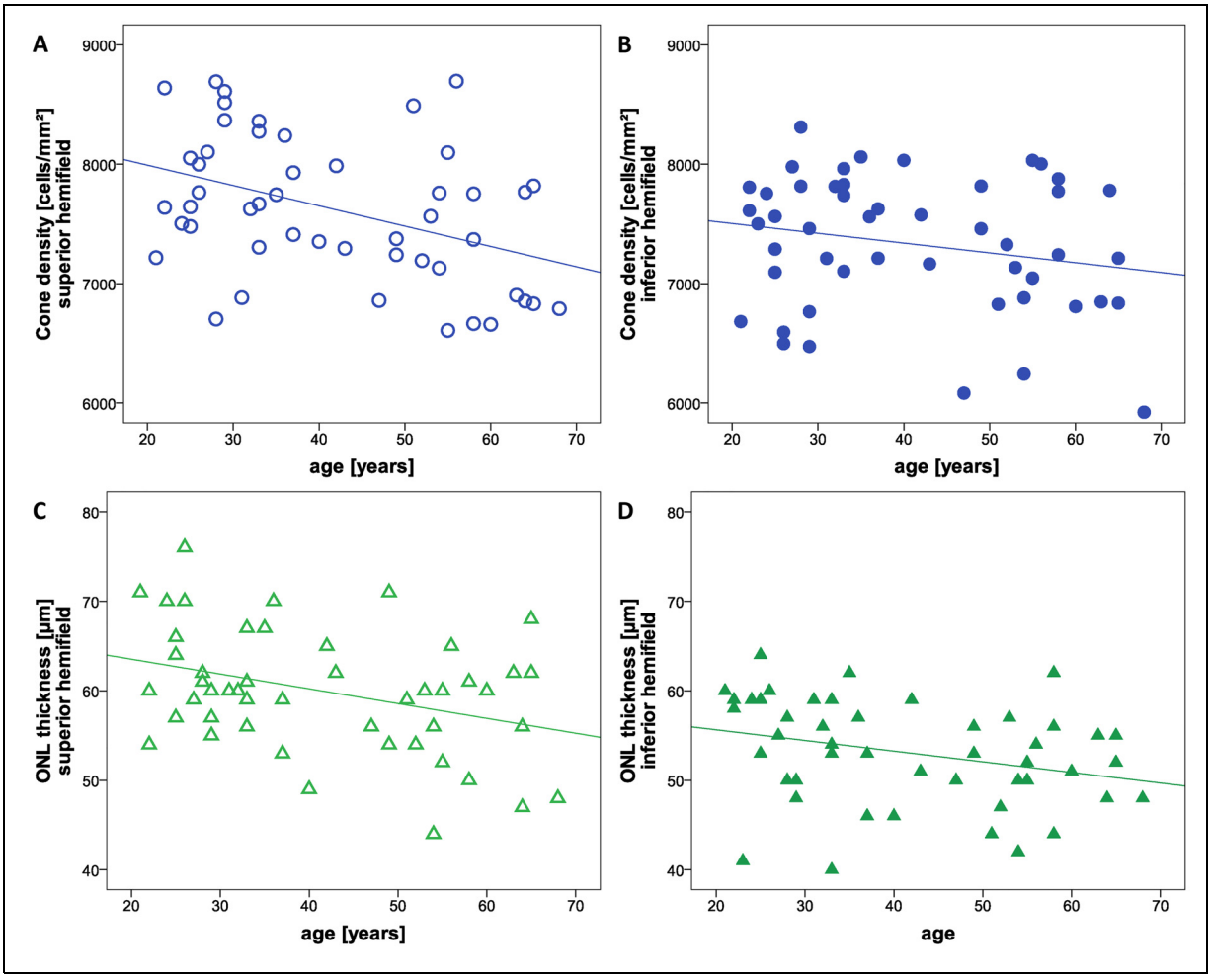

Figure 3. Cone density (a, b) and outer nuclear layer (ONL) thickness (c, d) as a function of participant age.
Relationship between local cone density/ONL thickness and age in the superior (a, c) and inferior (b, d) retinal hemifields.

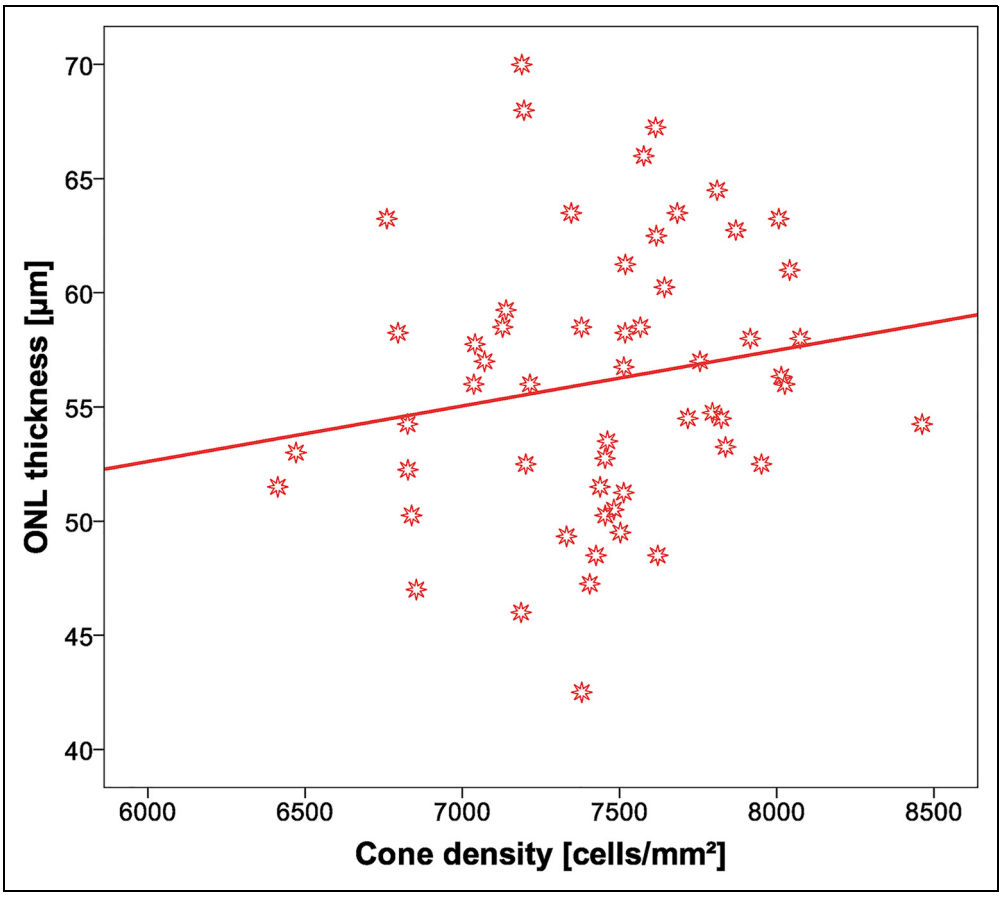

Figure 4. Relationship between cone density and outer nuclear layer (ONL) thickness. Cone density and ONL thickness data was averaged from all 4 quadrants.

largely independent of age and not significantly different between young and old participants beyond ~ 2 mm eccentricity.[16] In addition, the image quality of the cone images appears lower for older participants in comparison with younger participants in our study. Automated cone counting algorithms may not perform as well in poorer quality images; an inability to count all cones would result in an apparently lower cone density.

We did not find a relationship between cone density and ONL thickness. Menghini et al[13] reported that cone density was strongly correlated with ONL thickness between 0.5° and 1.5° eccentricity; however, this relationship weakens at more eccentric regions up to 3°. In our study, we measured beyond 3°, and it may be that there is even less (or no) association at greater eccentricities from the fovea. Another explanation may be that near the fovea, where cone density is much higher than elsewhere in the retina, the nuclei of the cones will be more compressed and stacked. Therefore, the greater the cone density, the thicker the ONL. Further away from the fovea, where cones are not so densely packed, the nuclei are also not densely packed, so the thickness of that layer should be more independent of cone density. As the cone array becomes sparse, so too do the nuclei, but the ONL thickness won't be affected by a meaningful amount.

Finally, it is important to consider if our images also captured rods and whether or not our cell density values include both rods and cones. We compared our cell counts with counts from published histology studies and found that our measures are in line with what would be expected only for conesat the test eccentricity.[7,20,21,23] In a study by Wells-Gray *et al,* AO-SLO images were acquired at various locations from 30° in the nasal retina to 30° in the temporal retina.[21] Cone density near the fovea was 164,000 cones/mm^2, decreasing to 6,700 cones/mm^2 at 30° in the nasal retina and 5,400 cones/mm^2 at 30° in the temporal retina. Peak rod density was 124,000 rods/mm^2 at 25° in the nasal retina and 120,000 rods/mm^2 at 20° in the temporal retina. At around 8° to 9° eccentricity, cone density was ~11,000 cones/mm^2 and rod density was ~ 8,500 rods/mm^2. Our cone count of 7,472 cones/mm^2 at 8.8° retinal eccentricity appears to be lower than in other studies including the AO study by Wells-Gray *et al.* Given our lower cone count and the much smaller diameter of rods, our technology is unlikely to be able to image rods either at 8.8° or any other retinal

location. Therefore, the visible pattern at this eccentricity is typical of cones alone.

Conclusion

In conclusion, we found a statistically significant negative correlation between cone density and age at 8.8° foveal eccentricity. ONL measured with SD-OCT at the same eccentricity was also significantly negatively associated with age, but the absence of a relationship between cone density and ONL thickness means that ONL is not a good surrogate for cone density at this eccentricity. The cone imaging technology described here and in our previous work may be a viable clinical alternative to AO technology when the resolution limit is not required to be above that for imaging cones. The data reported here are valuable for future studies of cone density with the HRA in which investigators wish to disentangle the effects of ocular disease and age.

Declaration of conflicting interests

The author(s) declared the following potential conflicts of interest with respect to the research, authorship, and/or publication of this article: J.M.: None; P.J.M.: Honoraria (Heidelberg Engineering); M.C.: None; N.S.: None; T.R.: Equipment loan (Heidelberg Engineering); S.C.D.: None; D.F.G.-H.: Lecturer (Heidelberg Engineering); Patent (ANSWERS; Moorfields MDT; T4); Equipment loan (Topcon; Heidelberg Engineering); R.S.A.: Travel funding (Heidelberg Engineering).

Funding

The author(s) disclosed receipt of the following financial support for the research, authorship, and/or publication of this article: The study was supported by Dr Hans and Mrs Gertrude Hirsch award from Fight for Sight UK to Tony Redmond and Roger S Anderson. Juliane Matlach received funding from Dr. Werner Jackstädt-Stiftung. Pádraig J Mulholland receives support from the College of Optometrists (UK), in the form of a Clinical Research Fellowship. David Garway-Heath is funded in part by the National Institute for Health Research (NIHR) Biomedical Research Centre based at Moorfields Eye Hospital and UCL Institute of Ophthalmology. David Garway-Heath's chair at UCL is supported by funding from the International Glaucoma Association. The sponsors or funding organizations named above had no role in the design or conduct of this research. The views expressed are those of the author(s) and not necessarily those of the NHS, the National Institute for Health Research, or the Department of Health.

ORCID iDs

Juliane Matlach https://orcid.org/0000-0002-2057-2191
Tony Redmond https://orcid.org/0000-0002-6997-5231

References

1. Wolsley CJ, Saunders KJ, Silvestri G, et al. Comparing mfERGs with estimates of cone density from in vivo imaging of the photoreceptor mosaic using a modified Heidelberg retina tomograph. *Vision Res* 2010; 50: 1462–1468.
2. Litts KM, Cooper RF, Duncan JL, et al. Photoreceptor-Based biomarkers in AOSLO retinal imaging. *Invest Ophthalmol Vis Sci* 2017; 58: BIO255–BIO267.
3. Godara P, Dubis AM, Roorda A, et al. Adaptive optics retinal imaging: emerging clinical applications. *Optom Vis Sci* 2010; 87: 930–941.
4. Carroll J. Adaptive optics retinal imaging: applications for studying retinal degeneration. *Arch Ophthalmol* 2008; 126: 857–858.
5. Marcos S, Werner JS, Burns SA, et al. Vision science and adaptive optics, the state of the field. *Vision Res* 2017; 132: 3–33.
6. Carroll J, Kay DB, Scoles D, et al. Adaptive optics retinal imaging--clinical opportunities and challenges. *Curr Eye Res* 2013; 38: 709–721.
7. Matlach J, Mulholland PJ, Cilkova M, et al. Relationship between psychophysical measures of retinal ganglion cell density and in vivo measures of cone density in glaucoma. *Ophthalmology* 2017; 124: 310–319.
8. Obata R and Yanagi Y. Quantitative analysis of cone photoreceptor distribution and its relationship with axial length, age, and early age-related macular degeneration. *PloS One* 2014; 9: e91873.
9. Park SP, Chung JK, Greenstein V, et al. A study of factors affecting the human cone photoreceptor density measured by adaptive optics scanning laser ophthalmoscope. *Exp Eye Res* 2013; 108: 1–9.
10. Song H, Chui TY, Zhong Z, et al. Variation of cone photoreceptor packing density with retinal eccentricity and age. *Invest Ophthalmol Vis Sci* 2011; 52: 7376–7384.
11. Aleman TS, Cideciyan AV, Sumaroka A, et al. Retinal laminar architecture in human retinitis pigmentosa caused by rhodopsin gene mutations. *Invest Ophthalmol Vis Sci* 2008; 49: 1580–1590.
12. Razeen MM, Cooper RF, Langlo CS, et al. Correlating photoreceptor mosaic structure to clinical findings in stargardt disease. *Transl Vis Sci Technol* 2016; 5: 6.
13. Menghini M, Lujan BJ, Zayit-Soudry S, et al. Correlation of outer nuclear layer thickness with cone density values in patients with retinitis pigmentosa and healthy subjects. *Invest Ophthalmol Vis Sci* 2014; 56: 372–381.
14. Mones J, Biarnes M, Trindade F, et al. Optical coherence tomography assessment of apparent foveal swelling in patients with foveal sparing secondary to geographic atrophy. *Ophthalmology* 2013; 120: 829–836.
15. Curcio CA, Messinger JD, Sloan KR, et al. Human chorioretinal layer thicknesses measured in macula-wide, high-resolution histologic sections. *Invest Ophthalmol Vis Sci* 2011; 52: 3943–3954.
16. Chui TY, Song H, Clark CA, et al. Cone photoreceptor packing density and the outer nuclear layer thickness in healthy subjects. *Invest Ophthalmol Vis Sci* 2012; 53: 3545–3553.
17. Jones BW, Watt CB, Frederick JM, et al. Retinal remodeling triggered by photoreceptor degenerations. *J Comp Neurol* 2003; 464:1–16.
18. Drasdo N and Fowler CW. Non-linear projection of the retinal image in a wide-angle schematic eye. *Br J Ophthalmol* 1974; 58: 709–714.

19. Li KY and Roorda A. Automated identification of cone photoreceptors in adaptive optics retinal images. *J Opt Soc Am A Opt Image Sci Vis* 2007; 24:1358–1363.
20. Mulholland PJ, Matlach J, Cilkova M, et al. Adaptive optics free photoreceptor imaging – comparison of manual and automated cone counts. ARVO Annual Meeting, 2016.
21. Wells-Gray EM, Choi SS, Bries A, et al. Variation in rod and cone density from the fovea to the mid-periphery in healthy human retinas using adaptive optics scanning laser ophthalmoscopy. *Eye (Lond)* 2016; 30: 1135–1143.
22. Muthiah MN, Gias C, Chen FK, et al. Cone photoreceptor definition on adaptive optics retinal imaging. *Br J Ophthalmol* 2014; 98: 1073–1079.
23. Curcio CA, Sloan KR, Kalina RE, et al. Human photoreceptor topography. *J Comp Neurol* 1990; 292: 497–523.
24. Anderson RS, Cilkova M, Mulholland PJ, et al. Effects of optical opacity on retinal cone counts measured by a narrow angle Heidelberg Retina Angiograph. ISIE Imaging Conference at ARVO, 2014.
25. Lujan BJ, Roorda A, Knighton RW, et al. Revealing Henle's fiber layer using spectral domain optical coherence tomography. *Invest Ophthalmol Vis Sci* 2011; 52: 1486–1492.